

# Experimental Study of Structural and Optical Properties of Copper Doped Tin Oxide Nanoparticles

K Bhuyan<sup>1,2</sup>, A Bhattacharjee<sup>3</sup>, D M. Bhuyan<sup>1</sup>, P R Alapati<sup>2</sup>

Associate Professor, Department of Physics, N Lakhimpur College, North Lakhimpur, India <sup>1</sup>

Research Scholar, Department of Physics, NERIST, Nirjuli (Itanagar), India <sup>2</sup>

Associate Professor, Department of Physics, NIT Meghalaya, Shillong, India <sup>3</sup>

Professor, Department of Physics, NERIST, Nirjuli (Itanagar), India <sup>2</sup>

**Abstract:** Tin oxide (SnO<sub>2</sub>) undoped and Cu doped nanoparticles were synthesized by chemical process using low-cost tin chloride as the starting material. The crystal structure, particle size and optical properties of the nano particles were investigated by X-ray diffraction (XRD), and UV absorption spectroscopy. The XRD pattern revealed the formation of SnO<sub>2</sub> and all the samples were found to be poly-crystalline in nature. The crystallite size for the undoped sample was calculated to be 11 nm approximately. The increase in doping concentration resulted in increase of the particle size and the size of the Cu doped samples were found to be in the 14 – 20 nm range. The UV-VIS studies showed decrease in band gap with increasing doping concentration.

**Keywords:** Semiconductor, nano-particles, SnO<sub>2</sub>, XRD, UV-VIS Spectroscopy, Crystallite structure, optical property

## I. INTRODUCTION

Tin oxide is an inorganic compound having white or off white colour and also sometimes found to be grey. It is a crystalline solid, diamagnetic in nature and is an amphoteric oxide. It is an n-type semiconductor having a wide band gap of about 3.6 eV [1]. It normally occurs as a rutile crystal with a tetragonal unit cell. It has a space group C<sub>2v</sub>, P4<sub>2</sub>/mm, and point group D<sub>4h</sub><sup>4h</sup>. In the rutile structure, the tin cations are surrounded by six oxide ions that form a slightly distorted octahedron. The oxide ions are coordinated by three tin cations in a planar geometry that is slightly distorted from the trigonal planer structure. Its lattice parameters are a=b=4.738 Å and c= 3.188 Å. It is a known fact that most electrical conductors are opaque and most optically transparent solids are electrically insulators. Electrical conduction in transparent solids occurs only in a few systems such as 4d metal oxides like SnO<sub>2</sub> and In<sub>2</sub>O<sub>3</sub>. SnO<sub>2</sub> is a prototype transparent conductor and it presents a high transparency in the visible range (above 90%) and high reflectivity in the infrared range in its undoped form [2]. This property is responsible for today's dominant use of SnO<sub>2</sub> as an energy conserving material [2]. The wide band gap makes SnO<sub>2</sub> an attractive matrix for electrically active emission [3] as wide band gap semiconductor has higher excitonic ionization energy. Owing to its unique chemical and physical properties such as high mechanical strength, chemical stability, resistance to oxidation, excellent adhesion, high optical activity and good thermal stability, it has immense potential in the field of such as photo-catalysis, transparent conducting electrodes for flat panel displays and solar cells, gas sensors and oxidation catalyst [4].

SnO<sub>2</sub> is one of the commonly used metal oxide semiconductors. Among differnt materials that are used in sensors, optoelectronic devices and transparent conducting oxides, the global market is dominated by metal oxide semiconductors. These metal oxide semiconductors can be easily used for fabrication of stable and high performance devices and intregated circuits. Metal oxides are cheap, abundant, green and quite versatile.

Nanomaterials have attracted wide interest in the fields of research and applications because of their novel physical and chemical characteristics which differ a great deal from the corresponding bulk materials. Compound semiconductors in nano scale have become an emerging field of studies due to the their innumerable applications. The extensive theoretical and applied research done on group III- V ( eg GaAs and InP) and group II- IV ( eg Cd chalcogenides) reveal that nano size semiconductor provide a solid base for the theory of semiconductor quantum dots. The wide band gap SnO<sub>2</sub> ( IVA- VIA) has also been a subject of interest owing to its multidimensional applications, especially its versatility as gas sensor [5, 6].

SnO<sub>2</sub> sensor performance (e.g., stability, sensitivity, and selectivity, etc.) has been improved considerably by reducing the size of the SnO<sub>2</sub> particles [7] and/or by adding dopants (typically noble metals or other metal oxides) to the tin dioxide[8]. SnO<sub>2</sub> has also been successfully doped with rare earth ions (Tb<sup>3+</sup>, Eu<sup>3+</sup>, and Ce<sup>3+</sup>) and transition metal ion (Mn<sup>2+</sup>) [9]. It has also been shown that several additives of metal ions like Al, Co, Fe, Cu can lead to the increase in the surface area of the SnO<sub>2</sub>

based powders [10]. With the advent of nanotechnology, the metal oxide semiconductors have been obtained as nanoparticles using methods like chemical vapour deposition[11], R.F magnetron Co- sputtering[12], laser pulse evaporation[13,14], Sol gel method[15,16], Spray Pyrolysis[17,18,19], and several other methods. These nanoparticles can be scaled to various sizes depending on the synthesis process. The nanoparticles of SnO<sub>2</sub> shows wide variation of properties depending on the size. In the present paper, pure and copper doped SnO<sub>2</sub> nano particles have been synthesized by chemical precipitation method. Cu has been doped with SnO<sub>2</sub> at concentration of 1% wt., 3% wt and 5% wt. Cu has been found to be very effective as a dopant in low concentration. The ionic radii of Sn<sup>4+</sup> are 0.069 nm and that for Cu<sup>2+</sup> is 0.073nm. Since the radii are comparable to each other, doping of Cu in SnO<sub>2</sub> occurs without any major alteration of the crystal structure. We also report an investigation of the optical properties of Cu doped SnO<sub>2</sub> with a view that it can potentially be used as an opto-electronic device.

## II. EXPERIMENTAL

All chemicals of AR grade were procured from Merck India Limited and were used without further purification. In order to obtain pure SnO<sub>2</sub> nano- particles, SnCl<sub>2</sub>.2H<sub>2</sub>O was mixed with ethanol and deionized water in a 5:11 ratio. The mixture was stirred for 5 minutes. HCl was gradually added in such a way that the colour of the solution just turns transparent. The solution was continuously stirred for about 15- 20 minutes. Aqueous ammonia was gradually added to the solution so that a pH of 8.5 was obtained. The precipitate was repeatedly washed with ethanol and deionized water so that chloride (Cl<sup>-</sup>) was completely removed. The precipitate was then extracted and is thoroughly dried until a fine white powder is obtained. Cu doped SnO<sub>2</sub> was obtained by a similar manner by adding CuCl<sub>2</sub>.2H<sub>2</sub>O to the starting solution so that the doping concentration of 1% wt, 3% wt and 5% wt is achieved. The XRD pattern of the prepared powder sample was obtained using a Rigaku Miniflex X ray diffractometer. Nickel filtered Cu K<sub>α</sub> line at 1.54 Å was used as the incident radiation and a scintillation detector was used to record the diffraction pattern. The obtained pattern was analysed using X'Pert High score software and was compared with the JSPDS database. UV visible studies were carried out using a Shimadzu UV2450 spectrophotometer with a powder sample attachment. The spectra were recorded from 200 nm to 900 nm.

## III. RESULTS AND DISCUSSION

The XRD pattern of the pure and doped samples of SnO<sub>2</sub> nano particles are shown in figure 1. It is to be noted that the XRD pattern of the doped and as well as the undoped samples correspond to the JCPDS card number 71-0652. No new peaks were observed in any of the patterns and nor any major peak shift was observable. This confirms the rutile structure of SnO<sub>2</sub>. EDS was performed using Oxford instruments model 7572 EDS

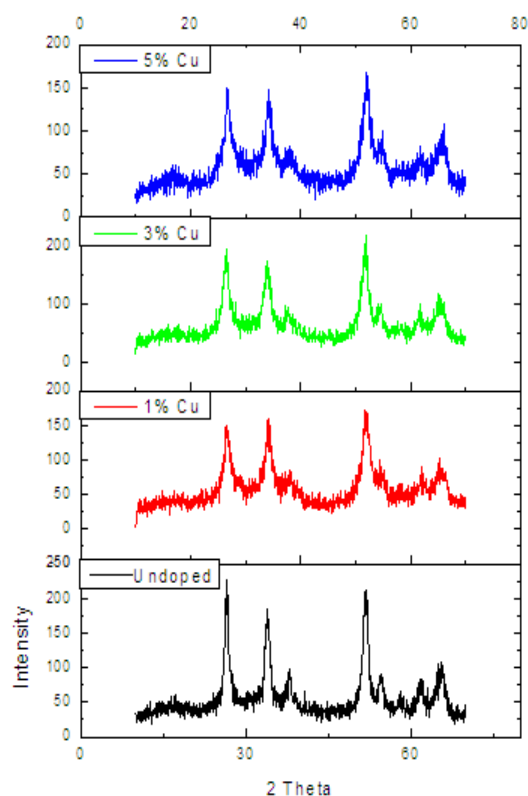


Fig. 1 XRD pattern of the pure and doped samples of SnO<sub>2</sub> nano particles

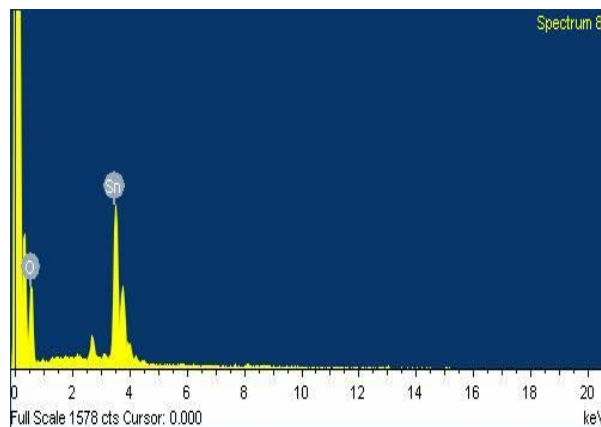


Fig.2(a) EDS spectra of undoped sample

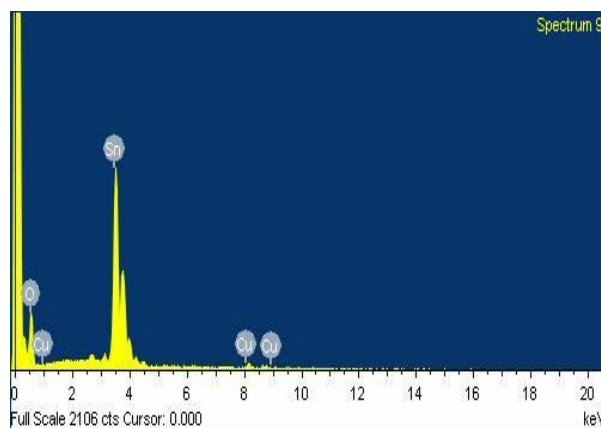


Fig. 2(b) EDS spectra of 1% copper doped sample

system. The EDS spectra are shown in figure 2(a), 2(b), 2(c) and 2(d). The EDS spectra confirmed that there were no impurities in the samples and the doped samples contained only Sn, O and Cu.

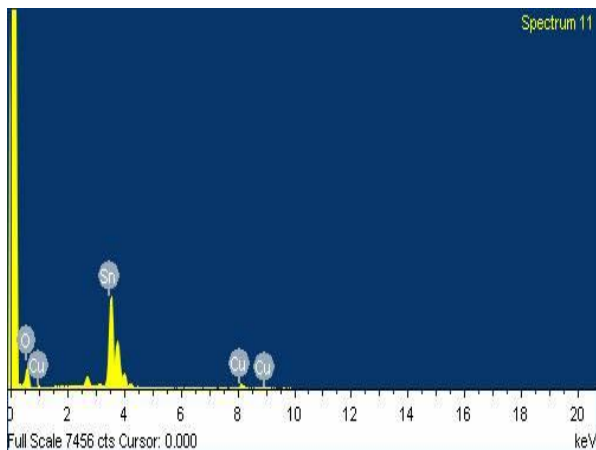


Fig. 2(c) EDS spectra of 3% copper doped sample

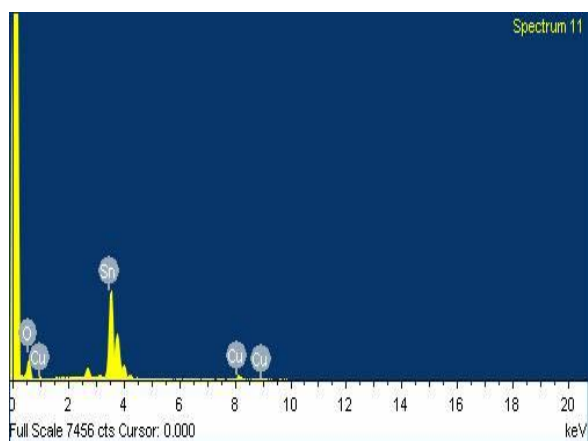


Fig. 2(d) EDS spectra of 5% copper doped sample

The intensity pattern of the compounds obtained from the XRD spectra showed a gradual decrease with doping concentration. This may be attributed to the fact that, the degree of polycrystallinity of the nano crystals has increased with doping. The peaks showed minor shifts in their positions with doping which indicates that with the doping of Cu into SnO<sub>2</sub>, some stress had developed within the lattice, but without any alteration to original rutile structure of SnO<sub>2</sub>. The Debye- Scherer formula was used for calculation of crystallite size which is given by,

$$D = \frac{K\lambda}{\beta \cos\theta}$$

where K is a constant whose value is 0.89, λ is the wavelength of X-ray radiation in nanometer, β is the full width at half maxima(fwhm) in radian and θ is the angle of diffraction in radian. The calculated values of the crystallite size are presented in table 1.

Williamson- Hall plot is a mathematical expression that relates the crystallite size to the broadening that is introduced by strain. This expression treats the peak width

TABLE I

CRYSTALLITE SIZE AS CALCULATED FROM DEBYE-SCHERER AND W-H PLOT

Samples	Crystallite size in nm		Strain
	Debye-Scherer	W-H plot	
Undoped SnO <sub>2</sub>	11.10144	12.0875	0.02187
1wt% Cu doped SnO <sub>2</sub>	14.79051	15.50863	0.01187
3wt% Cu doped SnO <sub>2</sub>	16.41763	18.627	0.00724
5wt% Cu doped SnO <sub>2</sub>	20.53139	23.72	0.00683

a function of the diffraction angle 2theta. The expression is represented as

$$\frac{\beta \cos\theta}{\lambda} = \frac{1}{D} + \frac{\epsilon \sin\theta}{\lambda}$$

where β is the FWHM in radians, λ is the wavelength of the incident X- ray in nanometers, D is the crystallite size in nanometer and ε is the strain induced due to doping. To construct the W-H plot sinθ/λ was plotted along the x axis and βcosθ/λ was plotted along the y axis. The inverse of the y-intercept gave the crystallite size where as the strain was directly obtained from the slope. The values of crystallite size and strain are also presented in table 1. The difference in size from the Debye-Scherer method can be attributed to the inclusion of strain that was introduced in W-H calculations. From table 1 it was observed that the crystallite size of the undoped SnO<sub>2</sub> nano particles are about 11nm and there has been a systematic rise in the crystallite size as the doping concentration Cu is varied from 1wt% to 5wt%. This may be due to the incorporation of Cu<sup>2+</sup> ion having a bigger radius (0.073nm) as compared to the radius of the host ion Sn<sup>4+</sup> (0.69nm) . The W-H plot reveals that the strain decreases with increase in doping, resulting in increase in the crystallite size in accordance with the equation β = εtanθ, where β fwhm, which increases as the crystallite size decrease, ε is the strain induced, θ is the angle of diffraction of the X ray and c is a constant. This confirms the increase of degree of polycrystallinity of SnO<sub>2</sub> due to the doping of Cu.

UV-Visible studies: It is well known that SnO<sub>2</sub> is a degenerate semiconductor having wide band gap energy (E<sub>g</sub>) in the range of 3.4–4.6 eV. The scatter in E<sub>g</sub> values of SnO<sub>2</sub> may be due to wide extent of non-stoichiometry of samples.

The dependency of the E<sub>g</sub> on the carrier concentration is explicitly reported in literature. It is reported that E<sub>g</sub> increases linearly with the increase in carrier concentration raised to the power 2/3 [20]. Measurement of diffuse reflectance with a UV-visible spectrophotometer is a standard technique in the determination of the absorption properties of materials if the grain size is in nanometres .The absorbance is given by Kubelka-Munk function or remission function expressed as,

$$F(R) = \frac{(1 - R)^2}{2R} = \frac{K}{S}$$

where R is reflectance. For determination of R two functions are required by using following relation

$$R = \frac{S}{K + S + \sqrt{K(K + 2S)}}$$

where K is absorption coefficient and S is scattering coefficient which is modified and used as absorbance function

$$F(R) = \frac{(1 - R)^2}{2R}$$

The optical absorbance coefficient  $\alpha$  of a semiconductor close to the band edge can be expressed by the following equation:

$$\alpha = \frac{\alpha_0 (h\nu - E_g)^n}{h\nu}$$

where  $\alpha$  is absorption co-efficient,  $E_g$  is the absorption band gap,  $\alpha_0$  is a constant, n depends on the nature of the transitions and values 1/2, 2, 3/2 and 3 corresponding to allowed direct, allowed indirect, forbidden direct and forbidden indirect transitions respectively. In the case of our samples, since we have a direct allowed transition, the value of n is taken as 1/2 ( $n = 1/2$ ). It is also a known fact that the absorption coefficient is proportional to absorbance and absorption is proportional to F(R), so we can write  $\alpha$  in place of F(R) or vice-versa. The UV-Visible spectra of the doped and the undoped samples are shown in fig 3. These spectra can be used to calculate the band gap in a semiconductor by plotting the square of absorbance as a function of  $h\nu$ .

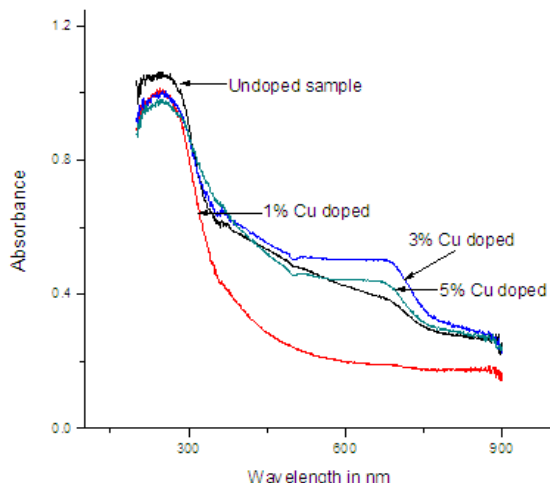


Fig. 3 UV Spectra of undoped sample along with doped samples

From the figure it is observed that the band gap decreases with increase in doping concentration. The values of the band gaps for the undoped and Cu doped nano particles, estimated from the graph is found is listed in table 2. The cut off wavelength is also calculated using the formula  $\lambda_c = 1.24/E_g \mu\text{m}$ . The decrease in band gap with increasing size confirms the effect of quantum confinement taking place. Similar decrease in band gap energy has been reported with other transition metals like Zn, Mg, Co and In [21]. The observed decrease in band gap can be attributed to the charge transfer transitions between the Cu ion s electrons and the SnO<sub>2</sub> conduction or the valance band.

TABLE II

BAND GAP AND CUT-OFF WAVELENGTH FOR PURE AND CU DOPED SnO<sub>2</sub>

Samples	Band gap $E_g$ in eV	Cut off wavelength $\lambda_c$ in $\mu\text{m}$
Undoped	3.421	0.362
1% wt Cu doped	3.259	0.380
3% wt Cu doped	3.207	0.387
5% wt Cu doped	3.168	0.391

The application of SnO<sub>2</sub> is found in low emission glass, electrodes, organic light emitting diodes, opto-electronic devices, lithium batteries, gas sensors, heat reflectors and polymer based electronics [22,23]. For visible LEDs, the most promising candidates are GaN ( $E_g = 3.44 \text{ eV}$ ) and related nitride semiconductors such as AlGaInN, which have direct band gap ranging from 1.95 eV to 6.2eV with corresponding wavelengths from 0.2 $\mu\text{m}$  to 0.63 $\mu\text{m}$ [24]. The values of the band gap of the undoped and Cu doped SnO<sub>2</sub> nanoparticles calculated from this study lie within this range. Thus they could find their utilization in these kinds of devices also.

#### IV. CONCLUSION

Undoped and varying concentrations of Cu doped nanoparticles are synthesized by chemical precipitation method and structural and optical characterizations were performed. The XRD study confirms the polycrystalline structure of the nanoparticles. The UV-VIS study confirms the quantum confinement effect. The range of band gap obtained from the studies is found to be suitable for opto electronic devices such as visible LED.

#### REFERENCES

- [1] C.Kilic, and A. Zunger, " Defects in Photovoltaic Materials and the origins of Failure to Dope Them", 2002
- [2] M. Batzili, U. Diebold, "The surface and material science of tin oxide", Progress in Surface Science, vol. 79, pp. 47-154, 2005.
- [3] A.J. Kenyon, Progress in Quantum Eletron, vol. 26,pp.225, 2002.

- [4] H. Zhu, D. Yang, G.Yu, H. Zhang, K. Yao, "Nanotechnology", vol. 17, pp. 2386, 2006.
- [5] A.A. Firooz, A.R. Mahjoub and A.A. Khodadai, "Highly sensitive CO and ethanol nano flower like SnO<sub>2</sub> sensors among various morphologies obtained by using single and mixed ionic surfactant templates", *Sensors and actuators, B: Chemical*, vol. 141, pp. 89-96, 2009.
- [6] F. Gu, S.F. Wang, M.k. Lu, Y.X. Qi, G.J. Zhou, D. Xu, and D. Youn, "Luminescent characteristics of Eu<sup>3+</sup> in SnO<sub>2</sub> nano particles" *Optical Materials*, vol. 25, pp. 59-64, Feb. 2004.
- [7] F. E. Krius, H. Fissan, and A. Peled, "Synthesis of Nanoparticles in the Gas Phase for Electronic, Optical and Magnetic Applications—A Review," *J. Aerosol Science*, vol. 29, issues 5– 6, pp.511–535, 1998.
- [8] E. Kanazawa, M. Kugishima, K. Shimano, Y. Kanmura, Y. Teraoka, N. Miura, and N. Yamazoe, "Mixed Potential Type N<sub>2</sub>O Sensor Using Stabilized Zirconia- and SnO<sub>2</sub>-Based Sensing Electrode," *Sens. Actuators B*, vol.75, pp.121–24, 2001.
- [9] L. M. Fang, X. T. Zu, Z. J. Li, S. Zhu, C. M. Liu, L. M. Wang, F. Gao, *J. Mater. Sci. Mater. Electron.* vol.19, pp.868-874, 2008.
- [10] H. Y. Jin, Y. H. Xu, G. S. Pang, W. J. Dong, *Mater.Chem. Phys.* Vol.85, pp.58-62, 2004.
- [11] P.M.Gorley, V.V.Khomyak, S.V. Bilichuk, I.G. Orletsky, P.P. Hovley and V.O. Gerchko, SnO<sub>2</sub> films:" Formation, Electrical and Optical properties", *Mater. Sci. and Engg. B*, vol. 118, pp.160-163, 2005.
- [12] K.S. Yoo, S.H.Park and J.H.Korg, " Nano-grained thin film Indium tin oxide gas sensors for H<sub>2</sub> detection", *Sensors and Actuators*, B, vol. 108, pp. 159-164, 2005.
- [13] H.T. Yang, and J.T. Cheung, "Pulsed Laser Evaporated SnO<sub>2</sub> films" *J. Crystal Growth*, vol.56, pp. 429-432, 1982.
- [14] H. Fang, T.M.Miller, H. Robert, M. Magruder and R.A. Weller, " The effect of strain on resistivity of Indium Tin Oxide film prepared by pulsed Laser deposition", *J. Appl. Phys.*, vol. 91, pp. 6194-6196, 2002.
- [15] O. Culha, M.F. Ebeoglugil, I. Birlik, E. Celik and M. Toparli, " Synthesis and Characterization of semiconductor tin oxide films prepared on glass substrate by Sol-Gel technique", *J. Sol-Gel Sci. Technol.*, vol. 51, pp. 32-41, 2009.
- [16] R. Ghosh, G.K. Paul and D.Basak, " Effect of thermal annealing treatment on structural, electrical and optical properties of transparent Sol-Gel ZnO thin films", *Material Research Bulletin*, vol. 40, pp. 1905-1914, 2005.
- [17] T. Serin, N. Serin, K. Karadeniz, H. Sari, T. Tugluoglu and O. Pakma, "Electrical, structural and optical properties of SnO<sub>2</sub> thin films prepared by spray pyrolysis", *Journal of Non-Crystalline solids*, vol. 352, pp. 209-215, 2006.
- [18] M. Oshima and K. Oshino, "Electron Scattering Mechanism of FTO Films Grown by Spray Pyrolysis Method", *Journal of Electronic Materials*, vol. 39, pp. 819-822, 2010.
- [19] J. Ouerfelli, S.O. Djobo, J.C. Bernede, L.Cattin, M. Mordily and Y. Berredjem, "Organic light emitting diodes using fluorine doped tin oxide thin films, deposited by chemical spray pyrolysis as anode", *Materials Chemistry and Physics*, vol. 112, pp. 198-201, 2008. Lu et al, "Carrier concentration
- [20] J.G Lue et al "Carrier concentration dependence of band gap shift in n-type ZnO:Al films", *J. Appl. Phys.*, vol. 101, 083705, 2007.
- [21] C. Drake and S. Seal, "Band gap energy modifications observed in trivalent In substituted nanocrystalline SnO<sub>2</sub>" *Appl. Phys. Lett.*, vol. 90, issue 23, 233117, 2007.
- [22] R.M. Agrawal, " H<sub>2</sub>S sensing properties of metal oxide (SnO<sub>2</sub>-CuO-TiO<sub>2</sub>) thin films at room temperature" *J. of Electron Devices*, vol.12, pp.730-73, 2012..
- [23] V. Subramanian, K. Gnanasekar and B. Rambabu, "Nanocrystalline SnO<sub>2</sub> and In-doped SnO<sub>2</sub> as anode materials for lithium batteries", *Solid State Ionics*, vol. 175, 181184 , 2004.
- [24] S. Nakamura and G. Fasol, *The Blue Laser Diode*, Wiley, New York, 1997.